IAHR AIRH

Journal of Hydraulic Research Vol. 00, No. 0 (2007), pp. 1–15

The effect of floodplain roughness on flow structures, bedforms and sediment transport rates in meandering channels with overbank flows:Part I

K. SHIONO, *Department of Civil and Building Engineering, Loughborough University, Loughborough, LE11 3TU, UK. E-mail: K.Shiono@lboro.ac.uk*

T. CHAN, *Atkins Water Peterborough, UK. E-mail: TuckLeong.Chan@atkinsglobal.com*

J. SPOONER, *Riley Consultants Limited, Auckland, New Zealand. E-mail: jake@jakespooner.co.uk*

P. RAMESHWARAN, *Centre for Ecology and Hydrology, Crowmarsh Gifford, Wallingford, Oxfordshire, OX10 8BB, UK. E-mail: ponr@ceh.ac.uk*

J. H. CHANDLER, *Department of Civil and Building Engineering, Loughborough University, Loughborough, LE11 3TU, UK. E-mail: J.H.Chandler@lboro.ac.uk*

ABSTRACT

Studies were carried out to understand the effect of floodplain roughness on flow structures, sediment transport rates and bedforms in a mobile meandering channel with overbank flows. Three floodplain roughnesses were examined in this study. Flow structures and bedforms were measured using a three component laser Doppler anemometer (LDA) system and digital photogrammetry, respectively. Comparisons of flow structures and bedforms between different floodplain rougheness are made. Considerable changes in the flow structure and bed form were observed. In particular, multiple secondary flow cells along the meandering channel occur at deeper water depths as the floodplain roughness increases. These cells also cause a series of wavy bedforms along the meandering channel. This paper is separated into two parts. Part I concentrates, in detail, on the flow structure with bedforms in the meandering channel for overbank flow as to change of floodplain roughness. The sister paper, Part II, concentrates on bed form formation during flood, sediment transport rates and flow resistance in the main channel and floodplain.

RÉSUMÉ

Keywords: Compound meandering channel, floodplain roughness, flow structure with bed forms.

1 Introduction

Flow mechanisms in compound meandering channels with fixed beds have been studied by many researchers, namely Mockmore (1943) and Shuky (1949), Ervine and Jasem (1989), Keily (1990), Willets and Hardwick (1993), Willetts and Rameshwaran (1996), Muto and Shiono (1998) and Shiono and Muto (1998) using relatively small flumes, and Sellin *et al.* (1993), and Greenhill and Sellin (1993) using a relatively large flume at the UK Flood Channel Facility (FCF). From those studies, there have been three main flow mechanisms observed: (1) the flow in the main channel below bankfull tends to follow the meandering main channel, while the floodplain flow generally follows in the valley direction and as a result horizontal and vertical shear are induced; (2) the secondary currents rotate in the opposite direction to that observed in inbank flows and energy loss due to the secondary currents in the main channel is greater than for an equivalent simple channel and (3) the flow on the floodplain outside the meander belt is usually faster than those within the meander belt, but its effect on the main channel flow resistance is relatively small.

There have also been few investigations into the flow structure in mobile meandering channels with straight floodplain walls for overbank flow. For example, Ishigaki *et al.* (2000)

demonstrated that secondary flow directly influences bedforms or vice versa. Ishigaki *et al.* also showed that the secondary flow has a significant impact on the distributions of primary flow and boundary shear stress that govern sediment movement in compound meandering channels. For sinuous floodplain walls, Okada and Fukuoka (2002) and Wormleaton *et al.* (2004) measured velocity and bedforms, and showed that secondary flow and bedforms are closely related. Bedforms have normally been measured using a pointer gauge across several cross sections along a meandering channel. This method loses details of the bedforms between the sections that could be important for an understanding of interaction between the flow and the bed. Photographs of bedforms along a channel are sometimes used to understand this interaction, however it is very difficult to depict details of the bedforms. In recent years, digital photogrammetric techniques have been developed to measure dense digital elevation models (DEMs) to capture bedform morphology along a channel (Chandler *et al.,* 2001). This research used this photogrammetry technique to measure the precise variation of the bedform along a meandering channel during flood conditions. This measurement together with detailed velocity measurements provided an insight into the interaction between bedform and flow, and also the effect of floodplain roughness on bedform and flow structure.

2 Experiment

Experiments were conducted in a 13 m long and 2.4 m wide flume with a fixed valley slope of 0.002. The flume had a two-stage meandering channel, consisting of a sinuous main channel and straight floodplain walls (see Figs 1 and 2). The floodplain was formed from 150 mm thick Styrofoam which was cut into shape and glued onto the flume basin. The main channel had a top width of 0.4 m, a sinuosity of 1.38 and was filled with uniform sand ($d_{50} = 0.855$ mm) so that the main channel depth was 40 mm. The depth of the sand was sufficient that the flume base was not exposed during the experiment runs. Flow circulation was facilitated by three recirculation pumps. One of which was a sediment recirculation pump which conveyed the sediments through the recirculation pipe system back to the inlet of the meandering channel. The water surface slope along the flume was controlled by three manual tailgates.

In this study, three floodplain configurations were assessed, with seven different flow rates. For these experiments, the floodplains were roughened with different roughness elements (see Fig. 1). The first experiment was a "smooth" floodplain that was made of Styrofoam. Paint was applied to ensure a homogeneous surface roughness and also to seal the channel. In the second set of experiments the floodplain was roughened with an 8 mm thick layer of artificial grass (golf putting grass) on the Styrofoam surface. In the third experiment the floodplain had a combination of artificial grass and rectangular concrete blocks. The rectangular concrete blocks were all identical (6.2×6.2 cm), and were laid in a square array with an additional block in the centre, which make a rhomboidal pattern having a spacing of 0.4 m $\times$ 0.4 m. These blocks were placed on the floodplain to simulate high roughness.

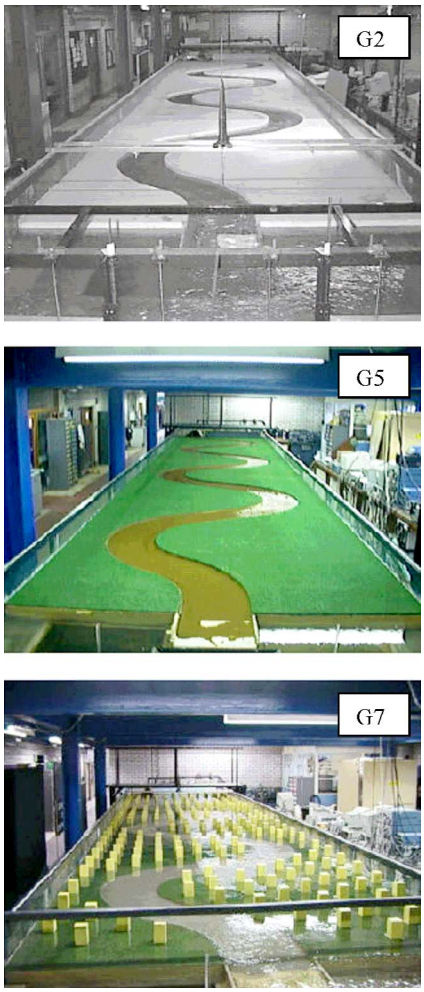

Figure 1 Pictures of floodplain roughness for G2, G5 and G7 cases.

For each of G cases examined the flume was intially run at bankfull depth and then increased incrementally for overbank depths. At each of the incremental flow depths, the flume was run for 36 h to allow the beforms to reach a quasi-equilibrium condition before each of the bedforms were measured. The complex morphological bedforms were recorded using digital photogrammetry (Chandler *et al.,* 2001) to a DEM resolution of 10 mm. The sediment transport rate was measured by collecting sediment discharge from the sediment recirculation pipe in 15–30 min intervals over a period of 6 h. The mean transport rate was calculated by averaging the transport rates over the whole collection period. Three-dimensional velocities were measured at several cross sections for several flow depths using a laser Doppler anemometer (LDA). Measurement cross sections for the LDA measurements are shown in Fig. 2.

3 Results and discussions

3.1 Stage–discharge

Stage–discharge data (H–Q) were collected over seven experiments that incorporated flat and mobile beds with various roughened floodplains (experiment numbers G1, G2, G3, G4, G5, G6 and G7). In this paper, three experiments (G2, G5 and

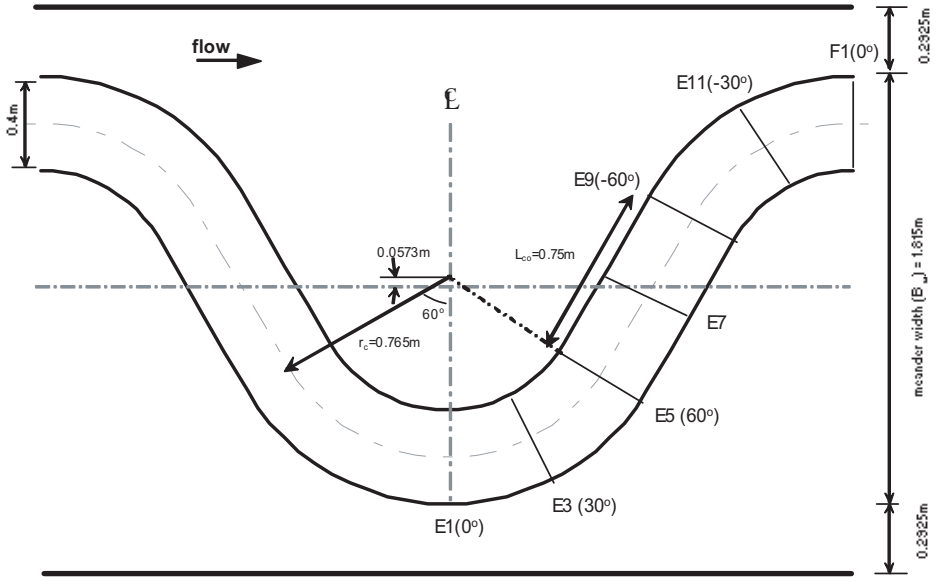

(a) Measurements sections

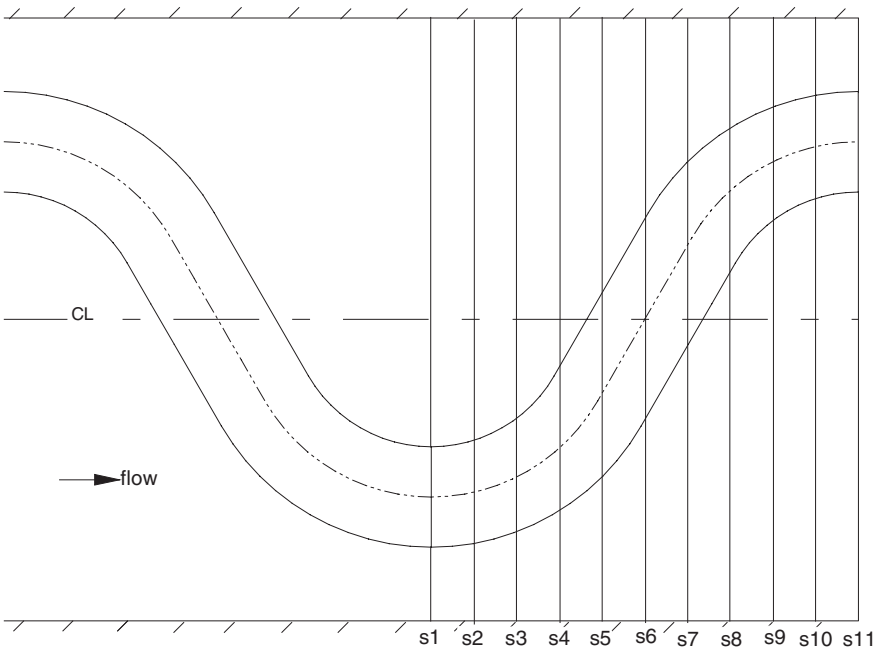

(b) Measurement sections at $Dr = 0.45$ for G2 case

Figure 2 Plan details of geometry and measurement sections for the test reach.

G7) with mobile bed were used to compare the relative characteristics of the H–Q curves and Table 1 shows those experimental conditions. Further details about the experimental set-up can be found in Chan (2003). The stage–discharge data for G2, G5 and G7 experiments are shown in Fig. 3. It is apparent from this figure that the discharge increases almost linearly with stage for inbank flow. It can be also seen that there is a discontinuity in the stage–discharge curve as the G2 experiment goes overbank. The reason for the discontinuity is the retardation of the main channel flow caused by slower floodplain flow entering the main channel as the floodplain is inundated. After the flow reaches a certain depth the stage–discharge relationship becomes approximately linear once again.

As for the influence of floodplain roughness on the overall discharge, the figure indicates that the smooth floodplain case (G2) was more efficient at conveying the water compared to the roughened floodplain cases (G5 and G7) as expected. For example, the smooth floodplain case conveys up to 50% more than the roughened floodplain G5 case at a total depth of 0.08 m ($Dr = 0.5$, Dr = floodplain water depth/main channel water depth), and

Table 1 Experimental conditions

Total width (m)	Meander belt width (m)	Main channel width (m)	Cross-over length (m)	Side slope S_o	Radius of curvature (m)	Sinuosity	Valley slope
2.4	1.815	0.4	0.75	90	0.765	1.3837	1/500
Series name	Main channel aspect ratio		Bed mobility	Roughness element		Sediment size d_{50}(mm)	
G2	10		Mobile	Smooth		0.855	
G5	10		Mobile	Grass		0.855	
G7	10		Mobile	Grass+blocks		0.855	

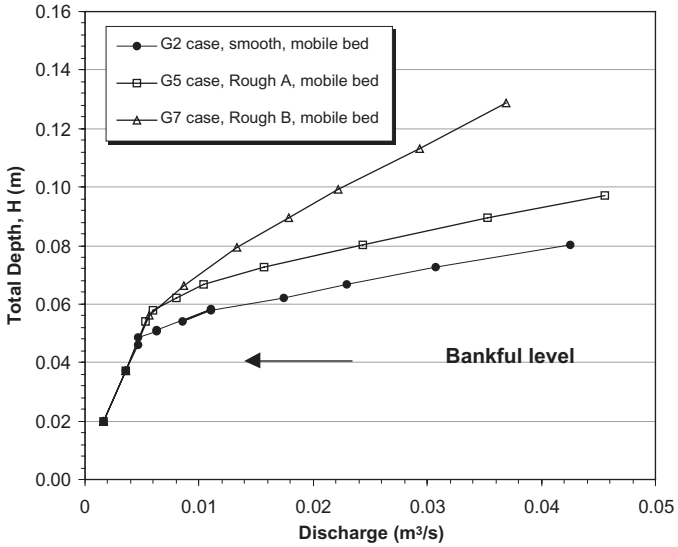

Figure 3 Stage–discharge relationships between mobile bed cases.

the conveyance efficiency reduces at higher flow stages for the roughened floodplain G7 case. In the block roughened floodplain case (G7), it is apparent that the stage–discharge curve increases linearly for water depths greater than 0.07 m ($Dr = 0.43$). Comparing the roughened floodplain cases, it can be seen that the rate of divergence between the grass and block floodplains is significant. However, the stage–discharge gradients between the smooth and grass floodplains are parallel. This implies that the flow resistance due to form drag of the blocks on the floodplain has a greater effect on the overall conveyance as the water depth increases. Thus under the block condition, the floodplain roughness is the dominant factor attributed to the overall discharge conveyance.

3.2 Velocity fields

The plan views of velocity vector field for G2 and G5 presented herein (Figs 4–8) are the depth-averaged velocities calculated over the depth in the main channel and floodplain. In the G7 case, the velocities at the apex section were only measured so that the full plan view of the velocity field is not able to be produced. To present a better picture of three-dimensional flow mechanisms in the mobile bed channel, the vector field was superimposed over the bedform elevations to demonstrate the interaction between the flow and the complex bedform in the main channel. The scale of the bed elevation is shown on the right hand side of each figure.

3.2.1 Smooth floodplain G2

For the bankfull case, Fig. 4 shows that a faster and deeper section appears along the outer bend with sediment deposition in the inner bend. This is a typical profile representing a meandering natural channel flow. The sediment deposition forms a point sand bar that extends along the mid channel to the cross-over section. Between the sand bar and the left-hand bank there is a flatter section where a little sediment transport has occurred. This is due to slow velocities in this region as shown in the figure. For overbank flow, $Dr = 0.3$, Fig. 5 shows that the faster and deeper section still remains along the outer bend, but there is a noticeable change in velocity direction from the bankfull velocity direction. The direction is slightly offset from the meandering channel direction which shows the floodplain flow interacting with the main channel flow. For $Dr = 0.45$, (Fig. 6) there is a series of wavy forms in which the velocity in the deeper sections is faster than in the shallower sections. The directions of flow are more or less along the ridge directions, and not along the meandering direction.

3.2.2 Roughened floodplain G5

In the roughened floodplain case, the bedforms were nearly the same as the bankfull flow depth case up to a depth of $Dr = 0.45$, but after $Dr = 0.45$, the bedforms start to change. Hence the velocity fields for $Dr = 0.45$ and $Dr = 0.55$ are only shown here (Figs 7 and 8, respectively) for comparison between the smooth and rough floodplain cases.

From Figs 6 and 7 for $Dr = 0.45$, it is clear that overall velocity on the rough floodplain is slower than on the smooth floodplain. The velocity in the main channel is also smaller. This shows a substantial retardation in the velocity in the main channel, which is due to much slower floodplain flow entering the main channel. Even at $Dr = 0.55$ (Fig. 8), the magnitude of the main channel velocity is still smaller than that of the smooth floodplain G2 case at $Dr = 0.45$. The bedforms have a series of ridges, but is not as regular as in the smooth floodplain case.

3.3 Internal flow structure at cross sections

From the previous sections it was seen that the magnitude of the longitudinal velocity in the main channel varies across the channel and along the meandering channel. The bed profiles also vary. The detailed internal flow structure along the meandering channel for overbank flows for the G2 case can be seen in Shiono *et al.* (2007). In this paper, the measured data were only plotted at two sections (cross-over section E7 and apex section F1) for G2, and

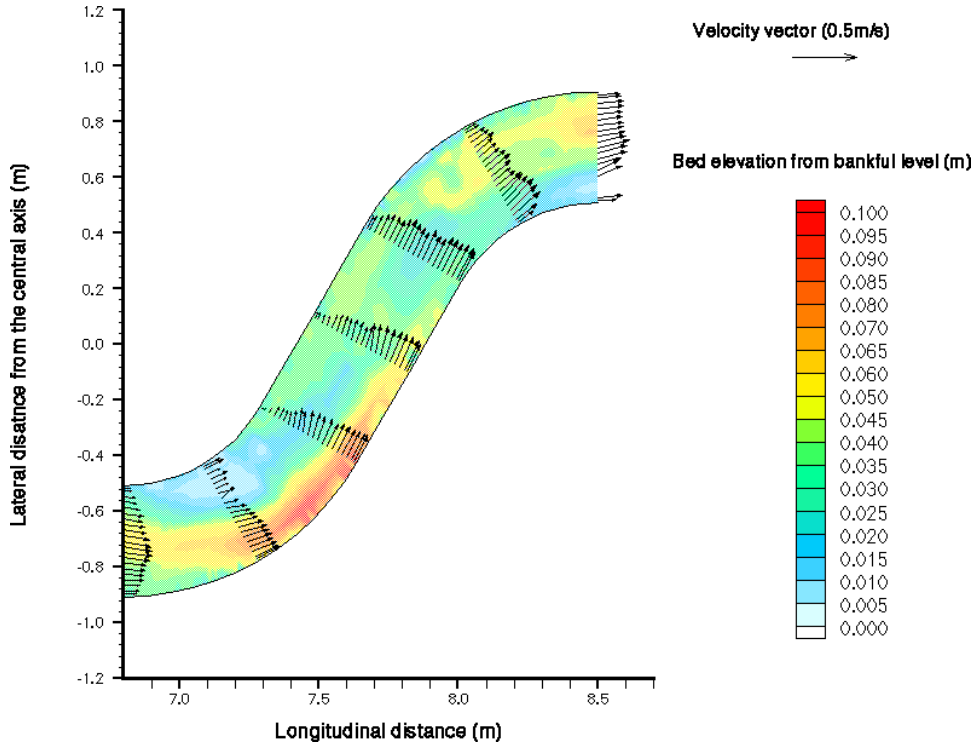

Figure 4 Velocity distribution at $Dr = 0.0$ (bankfull) for G2 case.

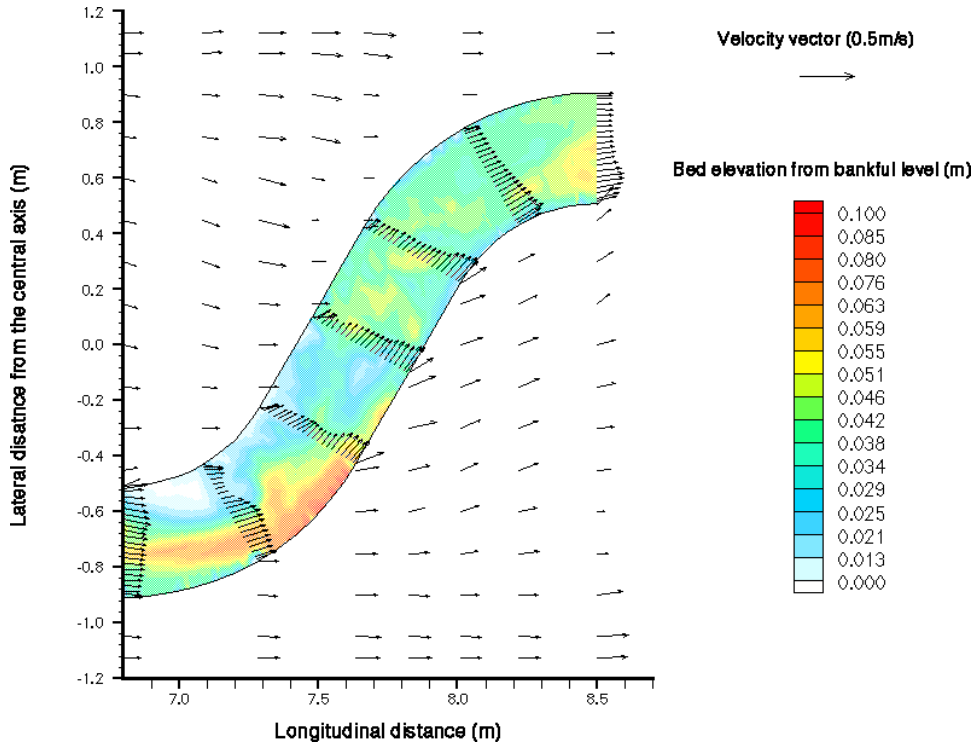

Figure 5 Velocity distribution at $Dr = 0.30$ for G2 case.

G5 and at F1 for the G7 case since the velocity measurements of G7 were only taken at apex section F1. All velocity distributions along the meandering channel for G2 and G5 cases can be found in Chan (2003).

3.3.1 Smooth floodplain

The flow pattern at the bankfull depth, in general, is typical for inbank flow, i.e. higher velocities mostly occur in the deeper regions and the lower velocities occur in the shallower regions (Fig. 9). The figure shows that the velocity maxima occur at about the mid water depth, not near the water surface as it does in straight open channels for a lage aspect ratio (Nezu and Nakagawa, 1993). In a straight narrow channel, a bulging pattern of the longitudinal velocity occurs near the corners of the channel, which corresponds well with the secondary flow directions caused by turbulence anisotropy. Looking at the longitudinal velocity and secondary flow at F1 in Figs 9 and 10, respectively,

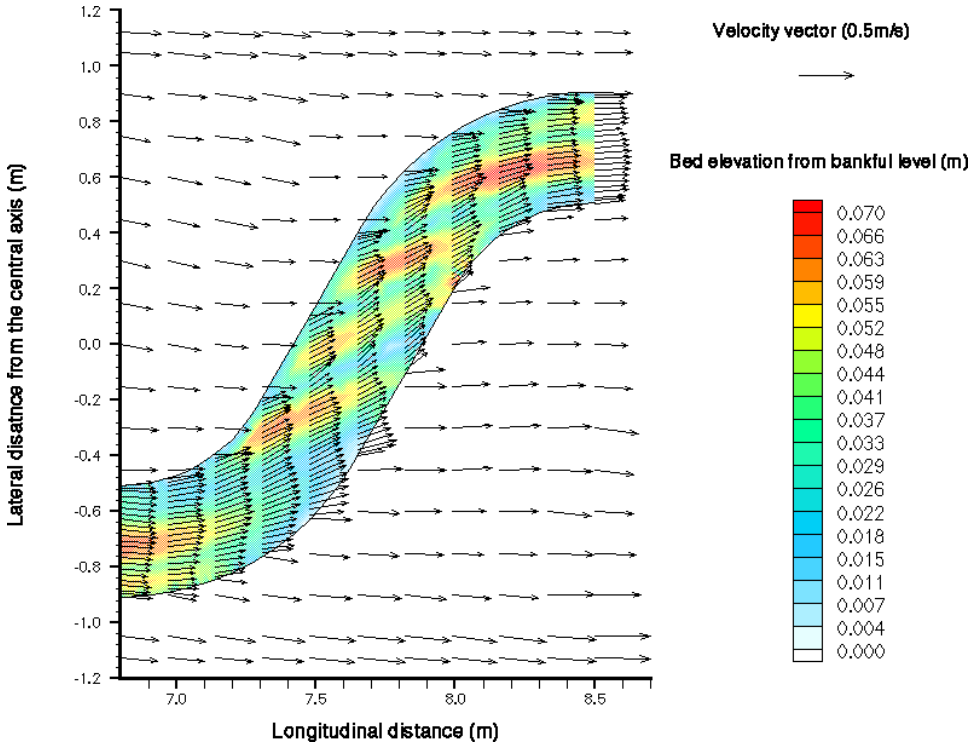

Figure 6 Velocity distribution at $Dr = 0.45$ for G2 case.

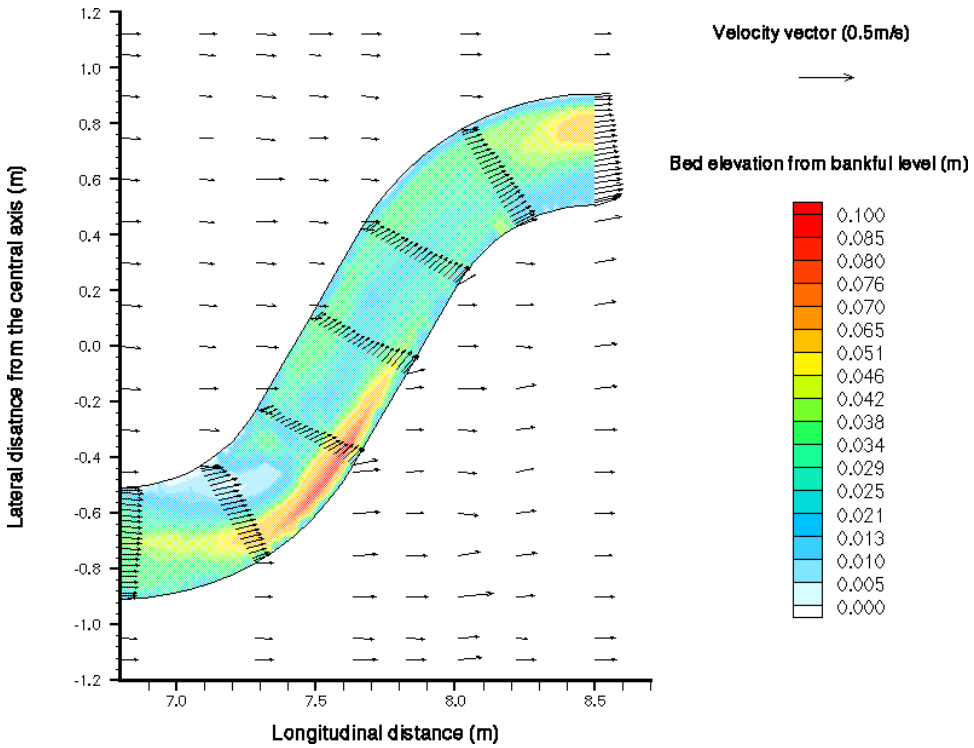

Figure 7 Velocity distribution at $Dr = 0.45$ for G5 case.

there are bulging flows, but they are not similar to straight channels, and the magnitude of the secondary flow is much larger than those generated by turbulence anisotropy. This suggests that the secondary flow generation is dominated by centrifugal force rather than turbulence anisotropy.

At $Dr = 0.3$, from Figs 11 and 12, distinctive flow patterns can be seen on the right-hand bank at cross-over section E7. Figure 12 shows that floodplain flow is entering the main channel. However the streamwise component of the floodplain velocity (see in Fig. 11) on the right-hand side is smaller than that of the main channel. This means that slower floodplain velocity effectively enters the main channel, as a result, the main channel velocity reduces. There is a strong clockwise secondary circulation below the bankfull level on the right side of the channel (see Fig. 12). On the left side of the deeper channel, there is faster and weaker clockwise circulation. Within the channel, there are a

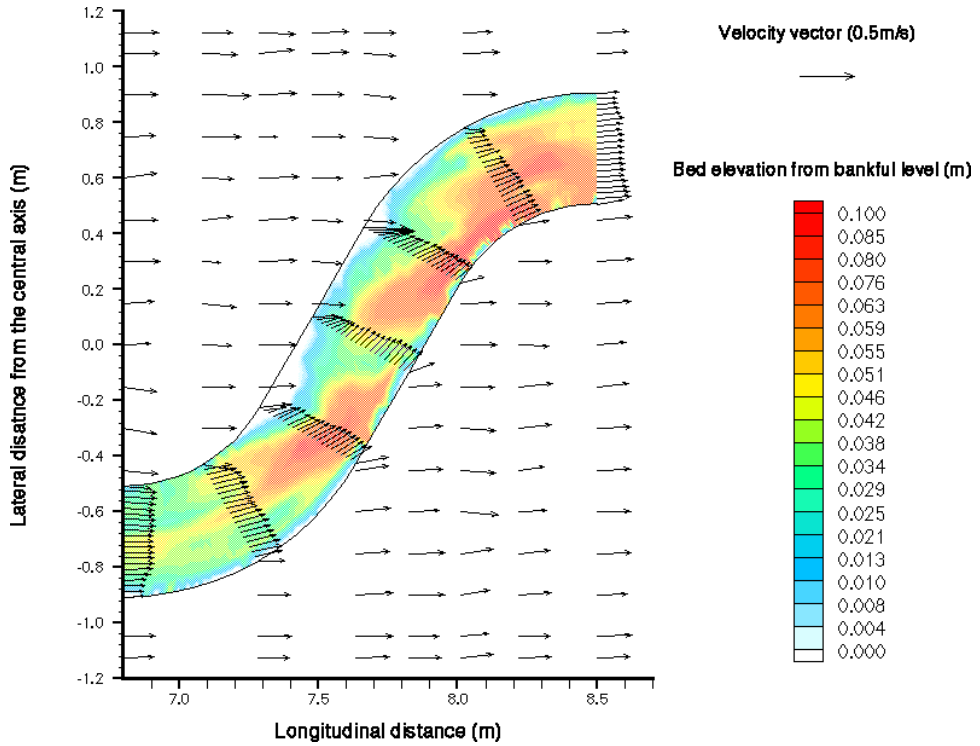

Figure 8 Velocity distribution at $Dr = 0.55$ for G5 case.

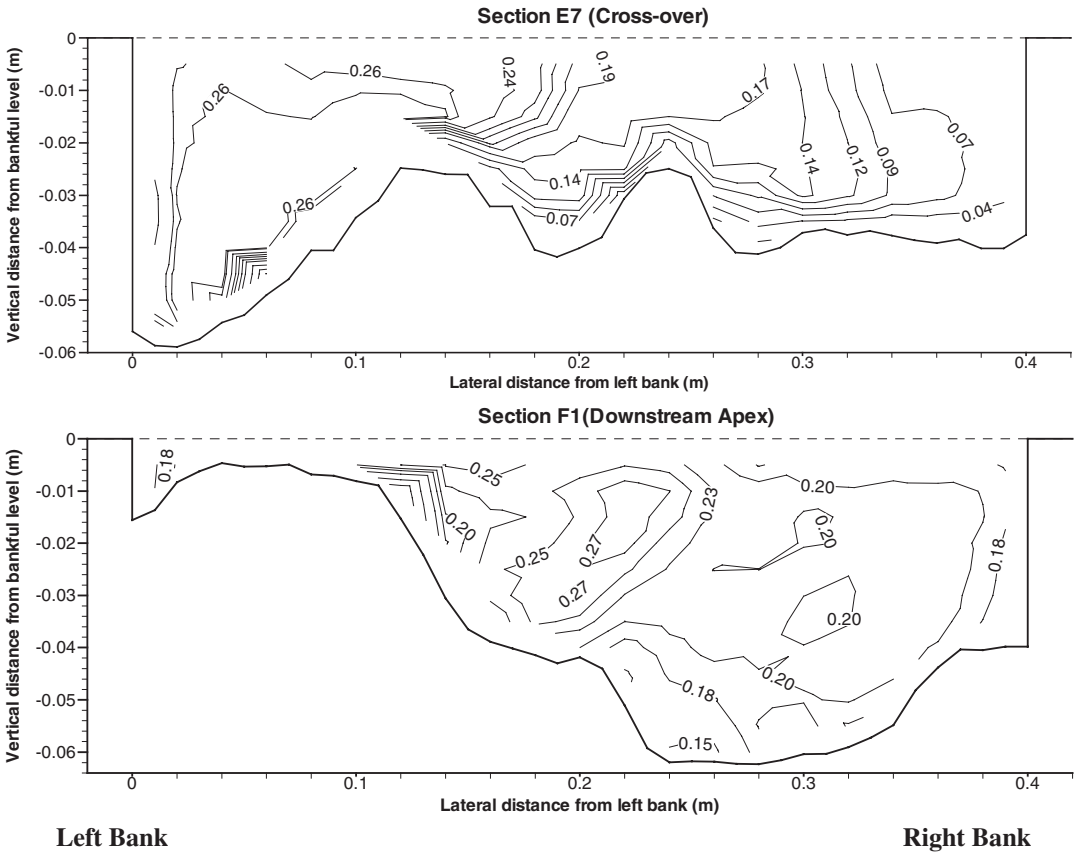

Figure 9 Longitudinal velocity distribution at $Dr = 0.0$ (bankfull) for G2 case.

number of maxima and minima and the large transverse and vertical gradients of velocity. At F1, on the left side of the channel there are the maximum velocity, a strong clockwise secondary circulation and floodplain flow entering the main channel above the bankfull level. There are relatively strong circular isovels and secondary flow on the left side of channel with the bedform pattern similar to the isovels. This suggests that bedforms, secondary flow and velocity are closely related.

Figures 13 and 14 show velocity and secondary flow at section 6 and F1 for $Dr = 0.45$. It should be noted that the cross section at

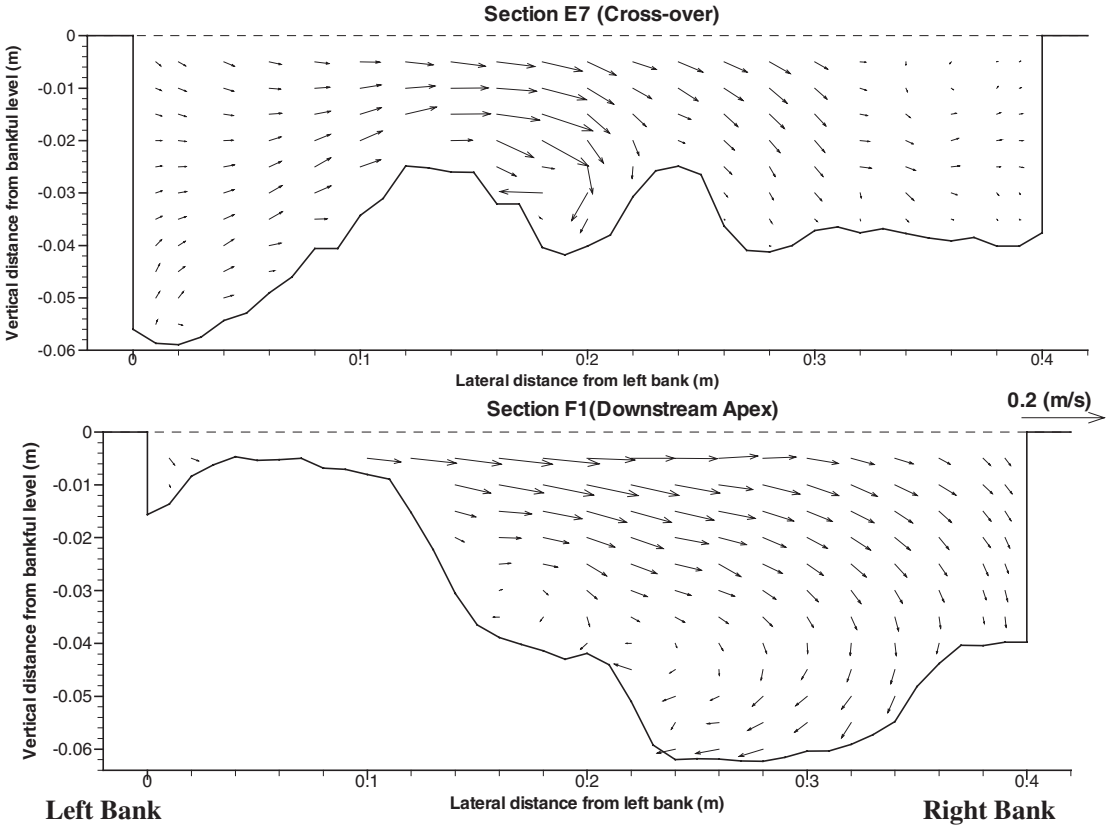

Figure 10 Secondary flow distribution at $Dr = 0.0$ (bankfull) for G2 case.

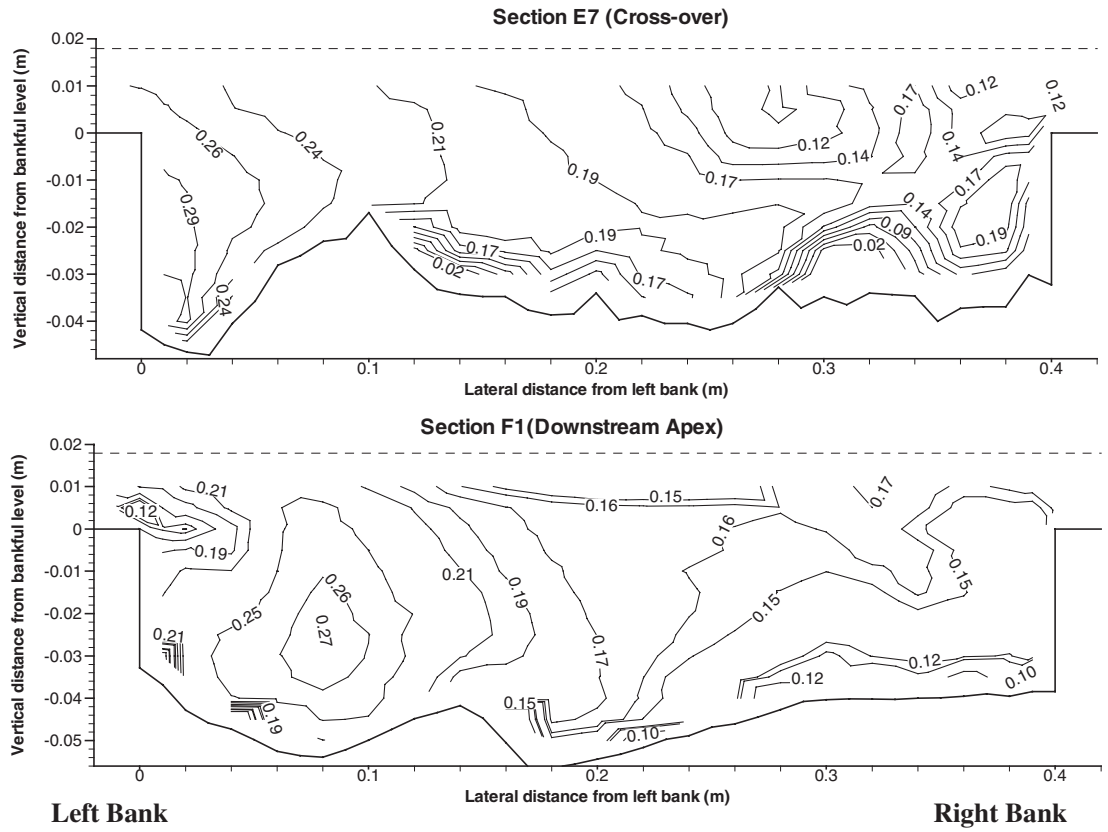

Figure 11 Longitudinal velocity distribution at $Dr = 0.30$ for G2 case.

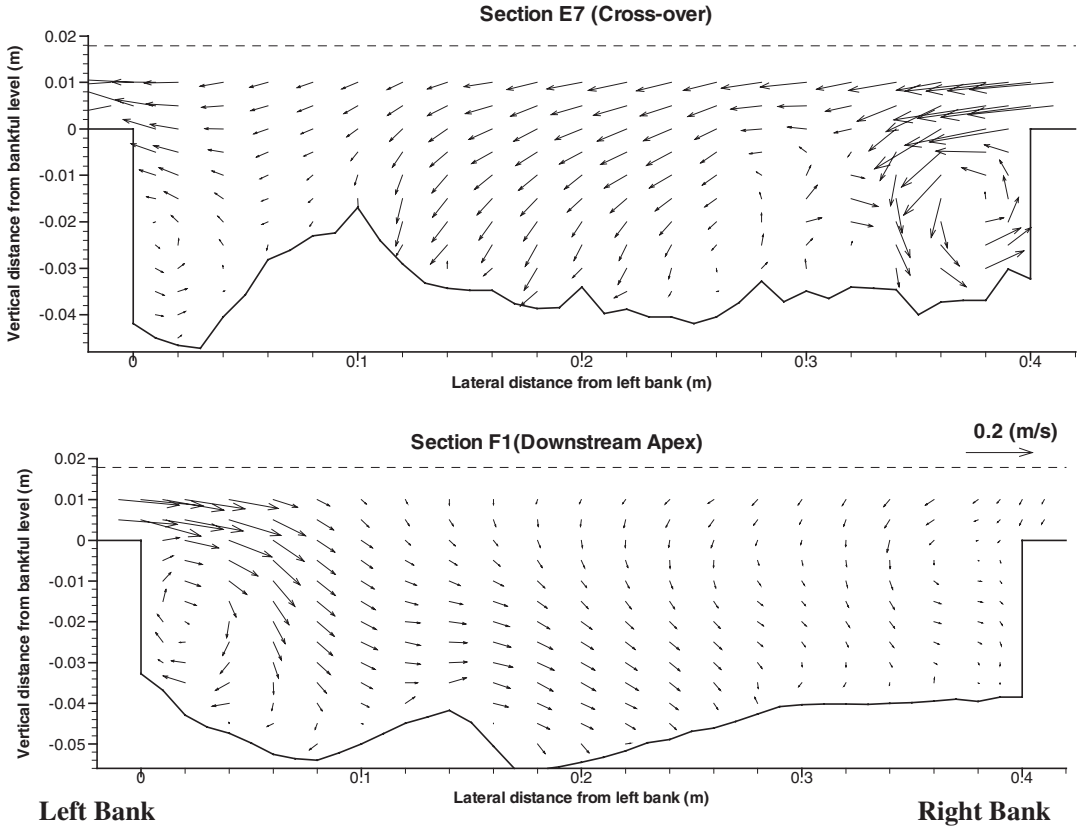

Figure 12 Secondary flow distribution at $Dr = 0.30$ for G2 case.

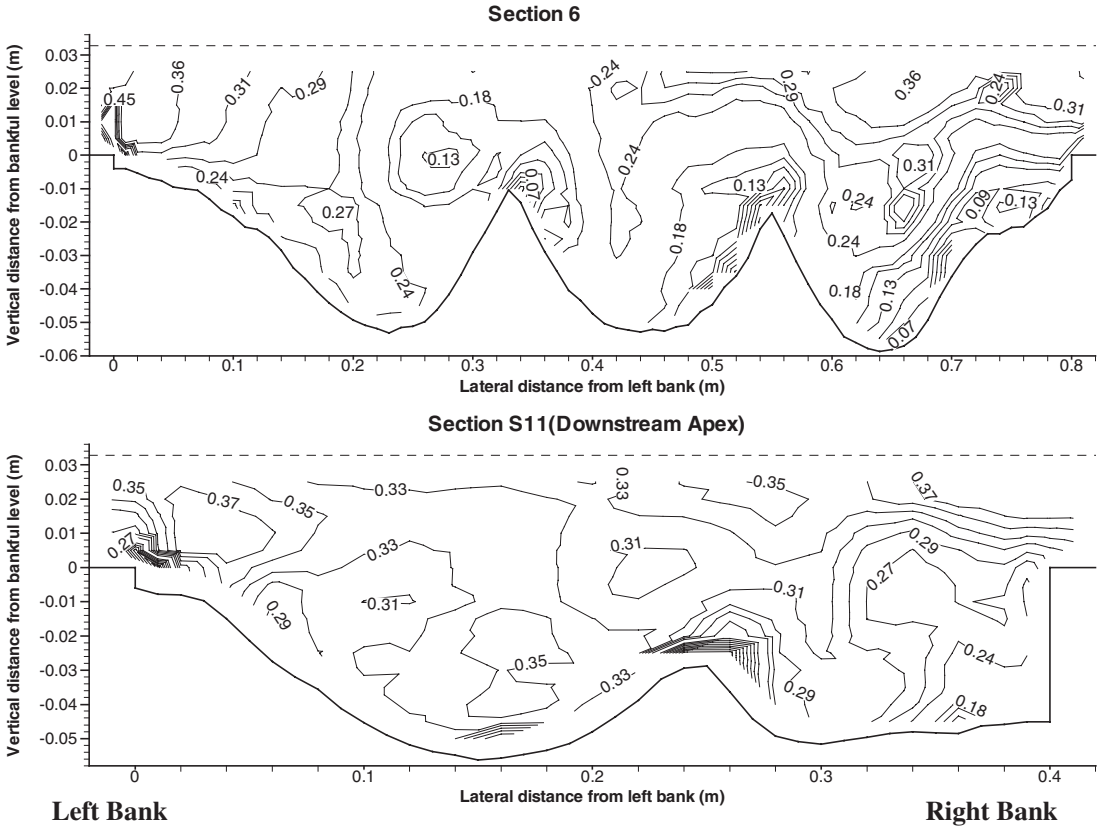

Figure 13 Longitudinal velocity distribution at $Dr = 0.45$ for G2 case.

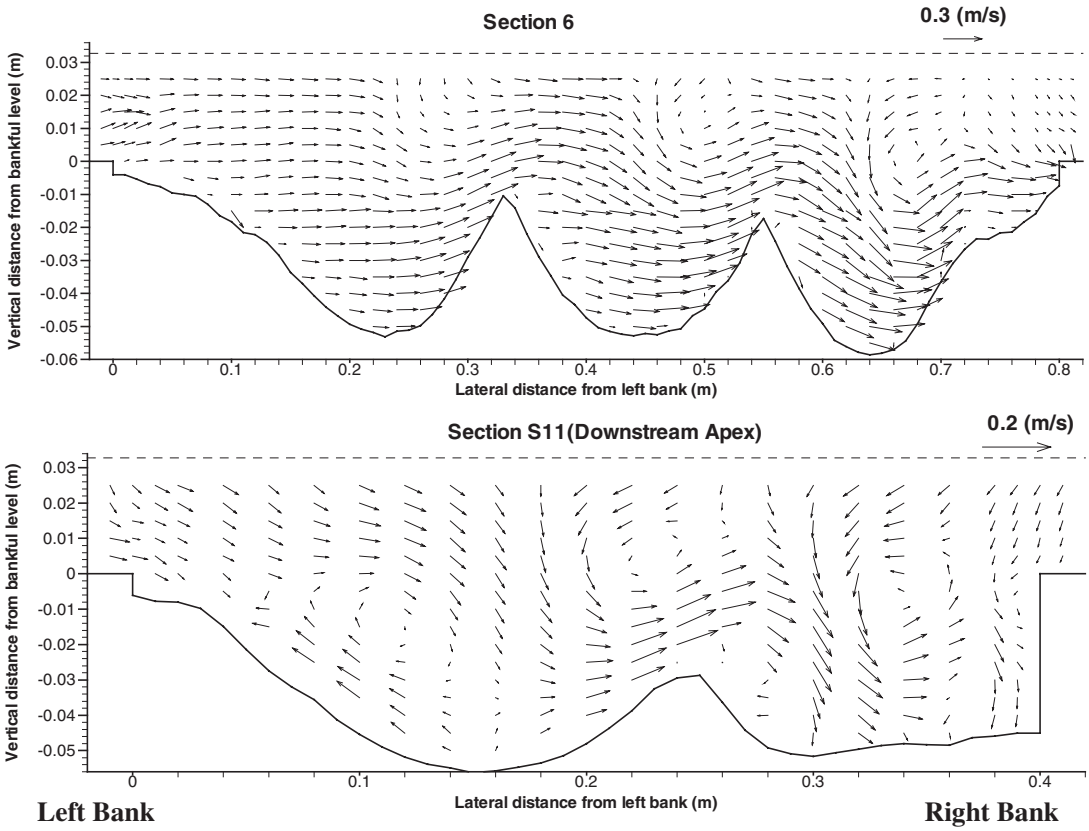

Figure 14 Secondary flow distribution at $D = 0.45$ for G2 case.

section 6 is perpendicular to the valley direction in the cross-over section (see Fig. 2(b)). The cross section is not perpendicular to the meandering channel as with the other relative water depth cases, hence the flow pattern is used as reference. In spite of the coordinate system at section 6, it can be seen that faster velocity occurs above the bankfull level on the right-hand side (see Fig. 13), which means that the flow below the bank level is accelerated due to faster floodplain flow. This generates a relatively large vertical gradient of velocity, as can be seen in the upper layer region. In Fig. 14, three anticlockwise secondary circulations in the upper layer above the wavy bedforms are clearly observed. At section F1, on the right side of the channel, faster velocities with large vertical gradients of velocity above the bankfull level are seen. Below that, there is a half circular isovel in which an anticlockwise secondary flow is situated (see Fig. 14). There are clockwise and anticlockwise circulations alternating across the section. The origin of these circulations was investigated by measuring velocities along one of the troughs. Figure 15 shows the secondary flow vectors along the trough, which indicates that the growth of secondary from the cross-over section, point A, to point D as shown by the decrease in the bed level along this reach and its decay from D to F as bed level increases. This suggests that these circulations originated in the cross-over section upstream and then developed along the ridges.

3.3.2 Roughened floodplain

The streamwise velocities and secondary flows in the main channel for the different relative depths of $Dr = 0.45$ and $Dr = 0.55$ in the rough floodplain G5 case are shown in Figs 16–19. At section E7 for $Dr = 0.45$ (Figs 16 and 17), there are two velocity maxima; on both banks, and also within anticlockwise circulations. This is similar to those at $Dr = 0.3$ for the smooth floodplain case. At F1, the maximum velocity occurs on the left side bank where the bed level is higher. The transverse velocity gradient exists across almost the whole cross section as can be seen in curved channel flow. Comparing velocity magnitudes between the smooth and rough floodplain cases at the same depth ($Dr = 0.45$), the velocity in the main channel is smaller for the roughened floodplain case and the floodplain velocity entering into the main channel is also smaller. This shows that slower floodplain flow due to floodplain roughness, enters the main channel and then retards the main channel flow considerably. As a result, the bedform still retains its inbank flow. In Fig. 17, it can be seen that there are two anticlockwise circulations above the bankfull level on the right side of the apex and one counter circulation underneath. As seen from Fig. 15, it is thought that those two anticlockwise circulations would be generated in the cross-over reach from upstream and carried downstream.

At section E7 for $Dr = 0.55$, Fig. 18 shows that distinct velocity maxima occur on the left side bank and near the bed in mid channel, on the other hand, distinct velocity minima occur above the maxima. There is also a significant small velocity on the right-hand side and the bed level is significantly higher than the initial bed level. In Fig. 19, strong floodplain flow enters the main channel from the right side of the bank. Two anticlockwise circulations are responsible for the shallower bed level and the velocity maximum and minimum at that region by the interaction between the floodplain and main channel flows. These secondary

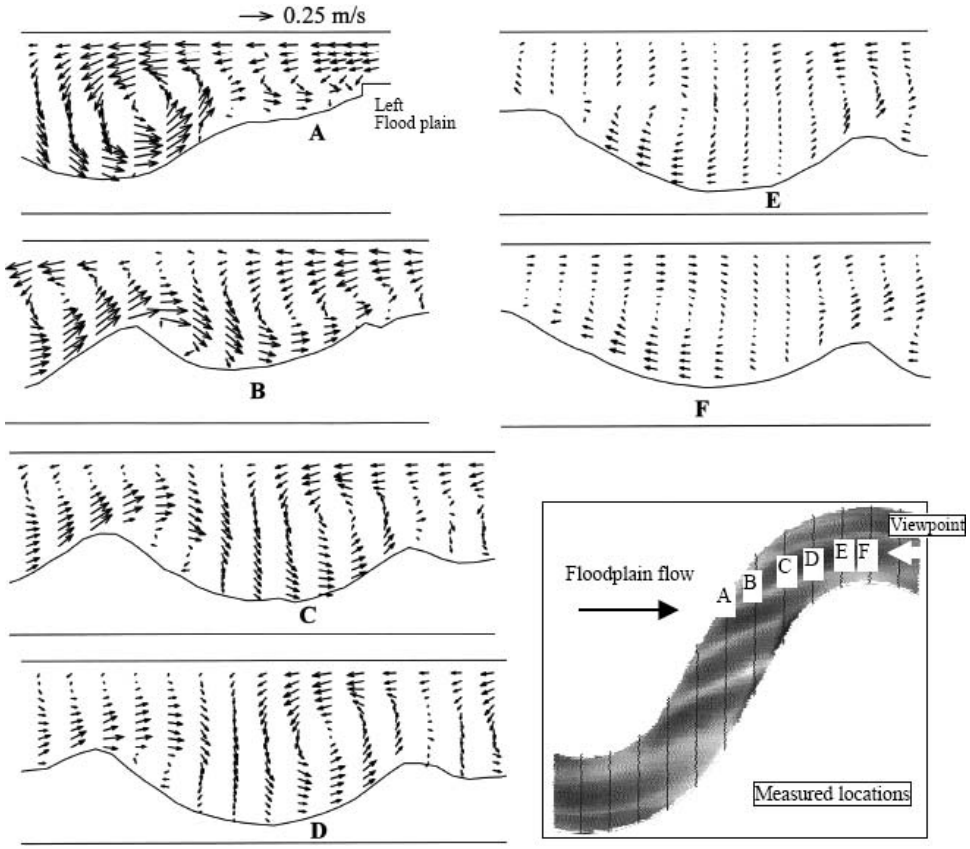

Figure 15 Development of secondary flow along a trough in the main channel.

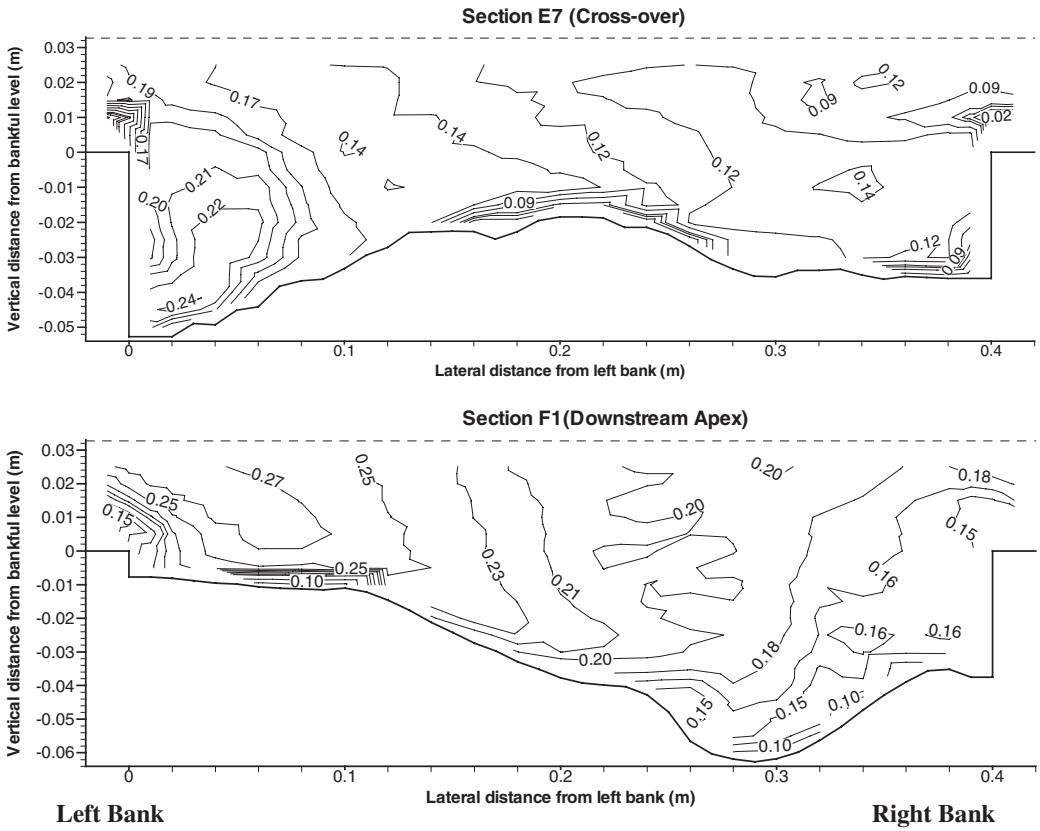

Figure 16 Longitudinal velocity distribution at $Dr = 0.45$ for G5 case.

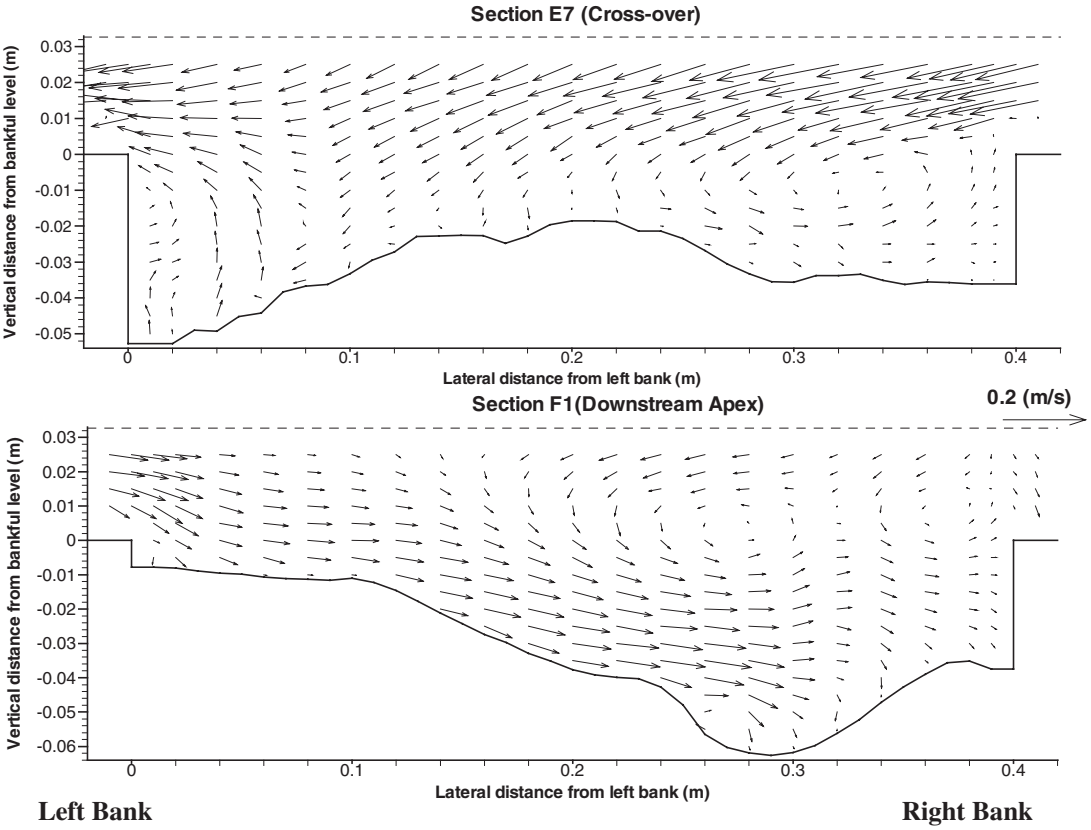

Figure 17 Secondary flow distribution at $Dr = 0.45$ for G5 case.

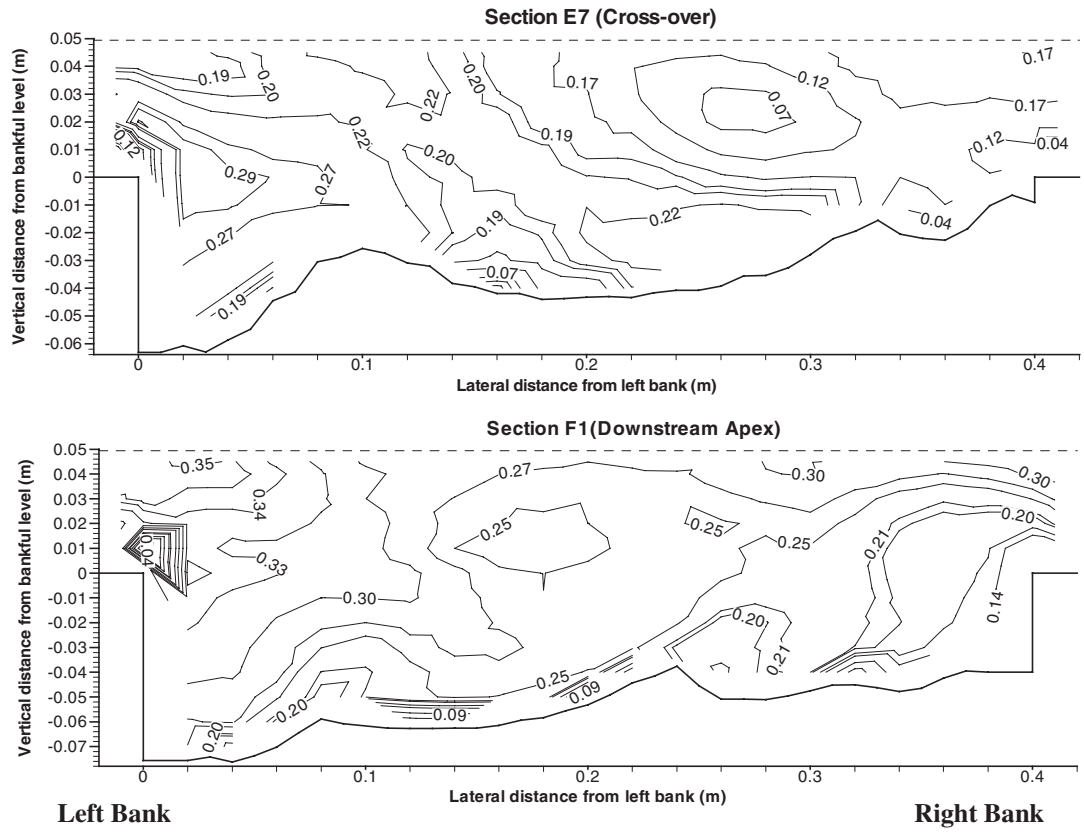

Figure 18 Longitudinal velocity distribution at $Dr = 0.55$ for G5 case.

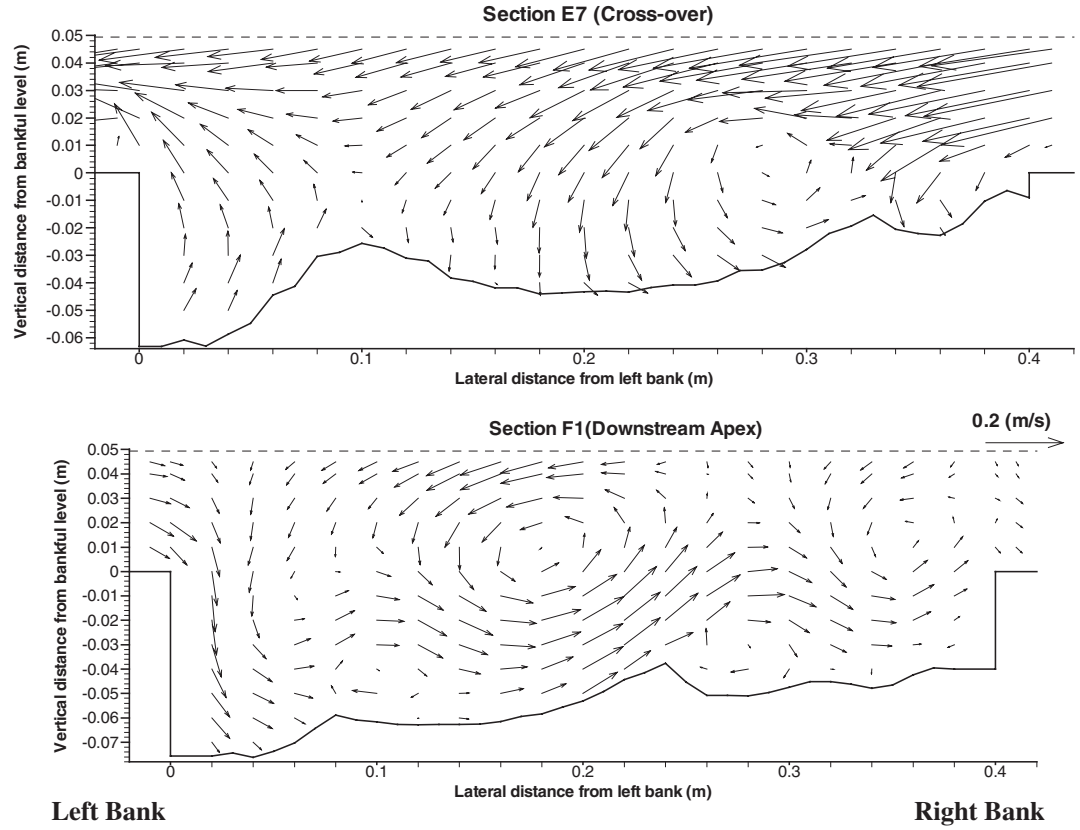

Figure 19 Secondary flow distribution at $Dr = 0.55$ for G5 case.

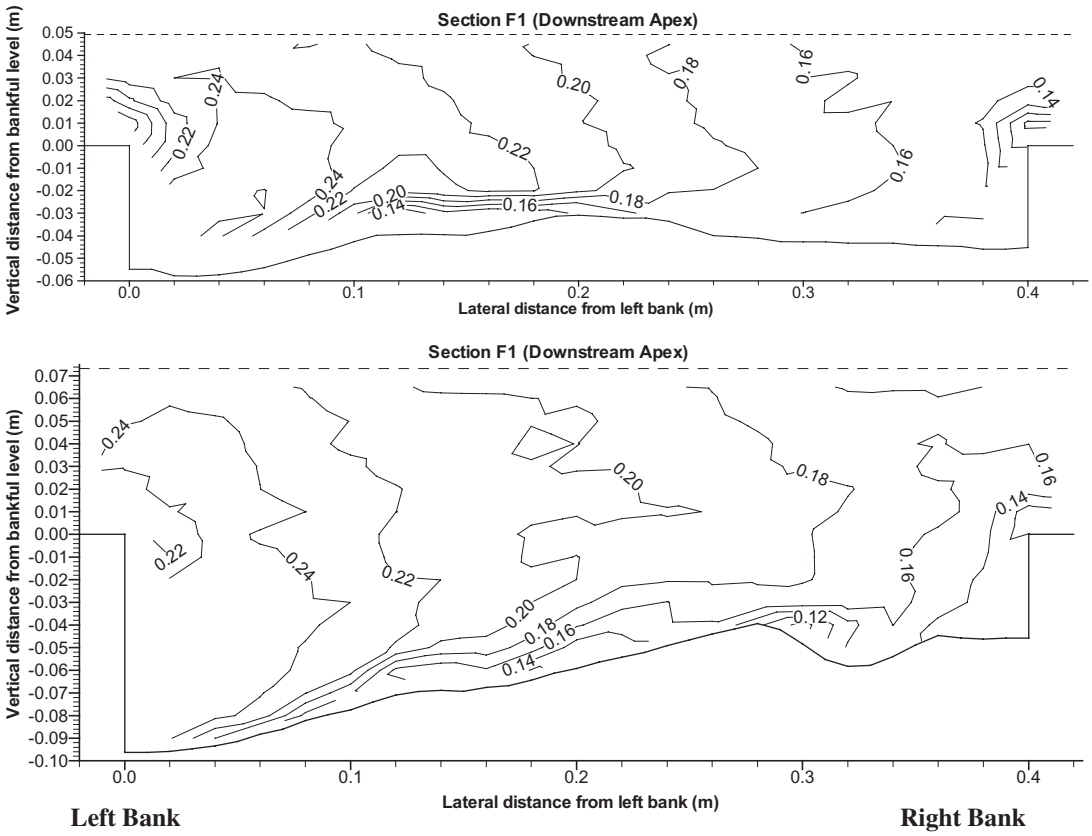

Figure 20 Longitudinal velocity distribution $Dr = 0.55$ and $Dr = 0.65$ for G7case.

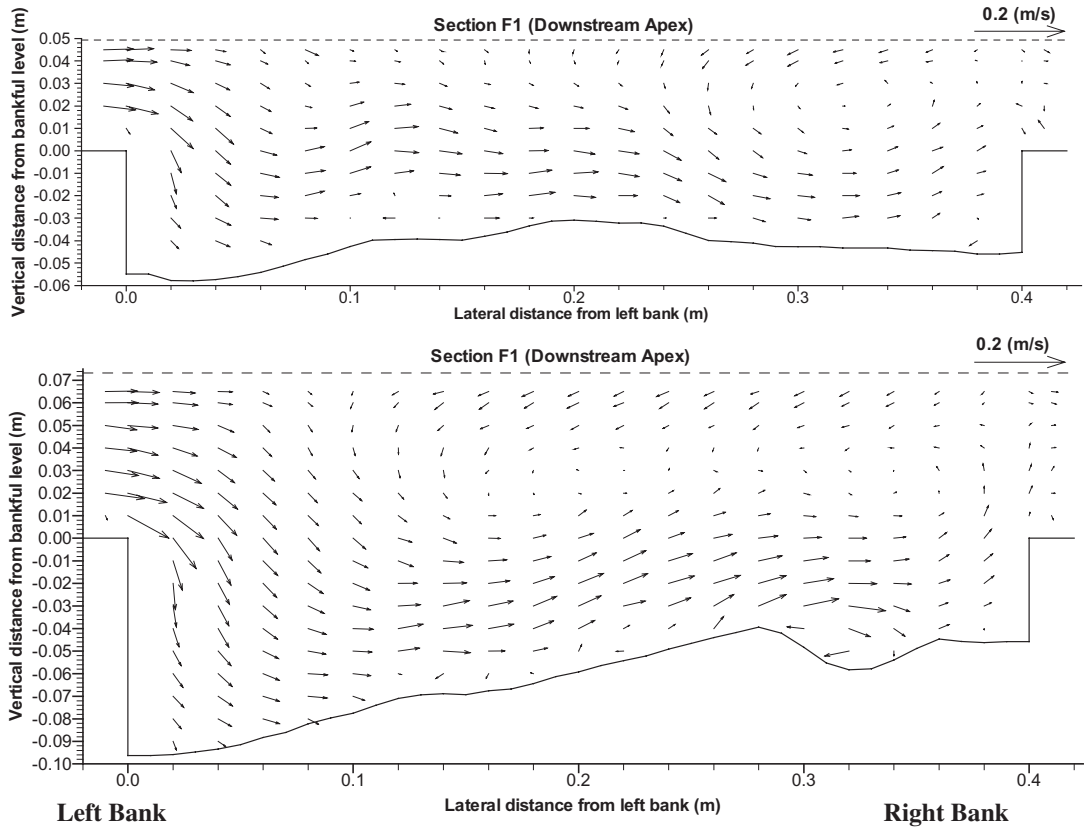

Figure 21 Secondary flow distribution at $Dr = 0.55$ and $Dr = 0.65$ for G7 case.

circulations are very similar to those of G2 at $Dr = 0.3$. On the left side of the bank, there is an anticlockwise circulation as occurred at $Dr = 0.3$ for the smooth floodplain G2 case and at $Dr = 0.45$ for case G5 as well.

In Fig. 18, at F1, the velocity is faster above the bankfull level than below, and the overall velocity is higher than in cross-over section E7, thus the flow accelerates from the cross-over to the apex. This phenomena was observed in all the cases studied. This indicates that the slowest flow along the meandering channel occurs at the cross-over section. There are alternative anticlockwise and clockwise secondary circulations across the section (see Fig. 19), but the anticlockwise ones are in the upper depth region and the clockwise ones are in the lower depth region. This flow pattern is very similar to that at $Dr = 0.45$ for the smooth floodplain G2 case. From Fig. 15 it is again thought that the anticlockwise ones would be generated in the cross-over section from upstream and transported downstream.

In the G7 case, the velocity measurements were only taken at apex section F1 for two water depths, $Dr = 0.55$ and $Dr = 0.65$. The velocity distributions and secondary flow vectors are shown in Figs 20 and 21. The velocity at $Dr = 0.55$ decreases from left to right, which is similar to that of G5 at $Dr = 0.45$. There is one established anticlockwise circulation in the upper layer, and a weak circulation on its left side. In the lower layer, the transverse component of velocity is crossing from left to right, which is also similar to that of G5 for $Dr = 0.45$.

For $i = 0.65$, the velocity decreases from left to right again and there are two anticlockwise circulations in the upper layer and two clockwise circulations near the bed, which is similar to those of G5 for $Dr = 0.55$. The velocity magnitudes at $Dr = 0.55$ is much smaller for G7 than for G5. From these flow structures it is clear that the secondary flow patterns for different roughened floodplains are more or less reproduced at different water depths.

4 Conclusions

The effects of floodplain roughness on main channel flow and bedforms in the compound meandering channel were investigated by laboratory experiments. The following conclusions are drawn.

During overbank flow, at $Dr = 0.45$ for the smooth floodplain case, multiple secondary flow circulations were observed together with regular wavy bedforms. There are three anticlockwise circulations in the upper region of the channel and clockwise circulations in the lower region at $Dr = 0.45$ for smooth floodplain case, at $Dr = 0.55$ for the rough floodplain G5 case and at $Dr = 0.65$ for the rougher floodplain G7 case. Similar flow and bed form patterns are reproduced at higher flow depths as the floodplain roughness increases. Bedforms and secondary flow circulations are therefore closely related.

Comparing the magnitude of velocities in the main channel between the smooth and roughened floodplain cases at the same depth, the velocities of the roughened floodplain cases are much slower than the smooth floodplain case, resulting from an increase in interaction between main channel flow and slower floodplain flow as the roughness on the floodplain increases. This is reflected in the stage discharge rating curves.

Although only three floodplain roughness cases were examined, clear evidence has been provided on the effect of floodplain

roughness on the flow structures and bedforms and as well on the stage discharge curve in the meandering channel for overbank flow.

Acknowledgments

This research was conducted as part of the EPSRC project GR/L69213 and the authors would like to acknowledge the EPSRC for their financial support. The second author is grateful to the Overseas Research Studentship Award (OSR) and Department of Civil and Building Engineering, Loughborough University for providing the scholarship for his study.

References

1. CHAN T.L. (2003). "A Study of Sediment Transport in Two-Stage Meandering Channel". PhD Thesis, Loughborough University.
2. CHANDLER, J., SHIONO, K., RAMESHWAREN, P. and LANE, S.N. (2001). "Measuring Flume Surfaces for Hydraulics Research Using a Kodak DCS460". *Photogram. Record* 17(97), 39–61.
3. ERVINE, D.A. and JASEM, H.K. (1989). "Flood Mechanisms in Meandering Channels with Floodplain Flow". *IAHR XXIII Congress*, The National Research Council Canada, pp. B449–B456.
4. GREENHILL, R.K. and SELLIN, R.H.J. (1993). "Development of a Simple Method to Predict Discharges in Compound Meandering Channels". *Proceedings of the Institution of Civil Engineers: Water, Maritime and Energy*, Vol. 101, pp. 37–44.
5. ISHIGAKI, T., SHIONO, K., RAMESHWARAN, P., SCOTT, C.F. and MUTO, Y. (2000). "Impact of Secondary Flow on Bed Form and Sediment Transport in Meandering Channels for Overbank Flow. *Ann. J. Hydraul. Eng.* Japan Society of Civil Engineers, 44, 849–854.
6. KIELY, G. (1990). "Overbank Flow in Meandering Compound Channels—The Important Mechanisms". *International Conference on River Flood Hydraulics.* W.R. White, Chichester, England, John Wiley & Sons, pp. 207–217.
7. MOCKMORE, C.A. (1943). "Flow Around Bends in Stable Channels". *American Society of Civil Engineers Papers*, pp. 335–360.
8. MUTO, Y. and SHIONO, K. (1998). "Three Dimensional Flow Structure for Overbank Flow in Meandering Channels". *J. Hydrosci. Hydraul. Eng.* 16(1), 97–108.
9. NEZU, I. and NAKAGAWA, H. (1993). "Turbulence in Open-Channel Flows". *IAHR Monograph*.
10. OKADA, S. and FUKUOKA, S. (2002). "Land-Form Features in Compound Meandering Channels and Classification Diagram of Flood Flows Based on Sinuosity and Relative Depth". *River Flow 2000*, Ed. Bousmar & Zech, pp. 205–212.
11. SELLIN, R.H.J., ERVINE, D.A. and WILLETTS, B.B. (1993). "Behaviour of Meandering Two-Stage Channels". *Proceedings of the Institution of Civil Engineers: Water, Maritime and Energy*, Vol. 101, pp. 99–111.
12. SHIONO, K. and MUTO, Y. (1998). "Complex Flow Mechanisms in Compound Meandering Channel for Overbank Flow". *J. Fluid Mechanic.* 376, 221–261.
13. SHIONO, K., SPOONER, J., CHAN, T., RAMESHWARAN, P. and CHANDLER, J.H. (2007). "Flow Characteristics in Meandering Channels with Non-Mobile and Mobile Beds for Overbank Flows". *J. Hydraul. Res. IAHR* (accepted).
14. SHUKRY, A. (1949). "Flow Around Bends in an Open Flume". *Trans. ASCE* 115, 751–788.
15. WILLETTS, B.B. and HARDWICK, R.I. (1993). "Stage Dependency for Overbank Flow in Meandering Channels". *Proceedings of the Institution of Civil Engineers: Water, Maritime and Energy*, Vol. 101, pp. 45–54.
16. WILLETS, B.B. and RAMESHWARAN, P. (1996). "Meandering Overbank Flow Structures. Coherent Flow Structures in Open Channels". ASHWORTH, P.J., BENNETT, S.J., BEST, J.L. MCLELLAND, and S.J. CHICHESTER (eds.) *England, John Wiley* and Sons, pp. 609–629.
17. WORMLEATON, P.R. SELLIN, R.H.J., BRYANT, T., LOVELESS, J.H., HEY, R.D. and CATNUR, S.E. (2004). "Flow Structures ina Two Stage Channel with a Mobile Bed". *J. Hydraul Res. IAHR* 42(2), 145–162.